Biomedical Materials

Deutsche Ausgabe: DOI: 10.1002/ange.201412129
Internationale Ausgabe: DOI: 10.1002/anie.201412129

Highly Biocompatible Nanofibrous Microspheres Self-Assembled from Chitin in NaOH/Urea Aqueous Solution as Cell Carriers**

*Bo Duan, Xing Zheng, Zhixiong Xia, Xiaoli Fan, Lin Guo, Jianfeng Liu, Yanfeng Wang, Qifa Ye, and Lina Zhang**

Abstract: *In this work, chitin microspheres (NCM) having a nanofibrous architecture were constructed using a "bottom-up" fabrication pathway. The chitin chains rapidly self-assembled into nanofibers in NaOH/urea aqueous solution by a thermally induced method and subsequently formed weaved microspheres. The diameter of the chitin nanofibers and the size of the NCM were tunable by controlling the temperature and the processing parameters to be in the range from 26 to 55 nm and 3 to 130 μm, respectively. As a result of the nanofibrous surface and the inherent biocompatibility of chitin, cells could adhere to the chitin microspheres and showed a high attachment efficiency, indicating the great potential of the NCM for 3D cell microcarriers.*

In tissue engineering, scaffolds are required typically to be biodegradable, biocompatible, and to have a porous three-dimensional (3D) structure with a nanotopography surface to mimic the extracellular matrix, which can provide sufficient space for cell adhesion, migration, and tissue formation.[1] Ma and co-workers have reported that nanofibrous hollow microspheres from poly(L-lactic acid) can efficiently accommodate cells and enhance cartilage regeneration.[2] Scaffolds composed of nanofibers can promote various functionalities of the cells and then direct cell migration and regeneration of tissues.[3] The fabrication of 3D nanomaterials has become the research focus of tissue engineering and regenerative medicine.[4] Recently, the micropatterning method using self-assembly or electrospinning techniques has been widely developed to create the "top-down" scaffolding 3D tissues.[1b,5] The "bottom-up" (from microscopic to macroscopic) tissue fabrication method has emerged as potentially powerful tool for the non-invasive reconstruction.[6] The microspheres based on natural polymers such as alginate,[7] chitosan,[6b] collagen,[6a] and PLLA[2] have shown great potential as cell microcarriers because of their advantage for in vivo observation of cells.

Chitin from natural resources, poly[β-(1,4)-*N*-acetyl-D-glucosamine], has been generally recognized to be nontoxic, biocompatible, and biodegradable,[8] and is promising for biomedical applications.[9] As an original component of living organisms, chitin is a good candidate for biomedicine materials.[8,9d,10] However, chitin is hardly soluble, only a few solvents have been acceptable for its dissolution including dimethylacetamide (DMAc)-LiCl,[11] $CaCl_2$-MeOH,[12] NaOH/urea,[13] ionic liquids,[14] and hexafluoroisopropanol (HFIP).[9a] For regenerated chitin nanomaterial fabrication, only chitin nanowhiskers obtained from ionic-liquid solvent,[9b] and a nanofiber film with excellent biocompatibility obtained from chitin solution in hexafluoroisopropanol (HFIP) have been reported by Rolandi and co-workers[9a,15]. In our previous work, chitin has been completely dissolved in NaOH/urea aqueous solution at low temperature to obtain a transparent solution, from which a series of biocompatible chitin-based aerogels, fibers, and hydrogels have been directly constructed.[16] However, the construction of homogeneous nanofibrous microspheres obtained by a totally different pathway has never been reported. On the basis that the NaOH hydrogen-bonded chitin complex was surrounded by the urea hydrates to form a water-soluble sheath-like structure adopting an extended chain, which led to chitin dissolution,[17] a violent fluctuation, for example, by high temperature, possibly destroyed the urea–NaOH sheath to induce the rapid aggregation of the stiff chitin chains in a parallel way, resulting in the formation of chitin nanofibers.

Herein, for the first time, we developed a novel approach for the direct construction of chitin-based nanofibrous microspheres (NCM) from chitin in NaOH/urea aqueous solution by thermally induced self-assembly. The urea–NaOH–chitin chain complex and its aggregates as nanofibers with a diameter ranging from approximate 4 to 12 nm co-existed in the dilute solution (see Figure S1 in the Supporting Information). At elevated temperature, the urea–NaOH sheath around the chitin was immediately destroyed, and the chitin chains quickly self-aggregated in parallel (with the largest contact area) through hydrogen bonding and hydrophobic interactions to form nanofibers with a mean diameter of approximate 27 nm (Figure 1b). The end hydroxy groups of chitin were attached to each other through hydrogen bonds, leading

[*] B. Duan, X. Zheng, L. Guo, Prof. L. Zhang
College of Chemistry & Molecule Science, Wuhan University
Wuhan, 430072 (China)
E-mail: zhangln@whu.edu.cn
Z. Xia, Prof. J. Liu
Sino-France Laboratory for Drug Screening
Key Laboratory of Molecular Biophysics of Ministry of Education
Huazhong University of Science and Technology
Wuhan, 430074 (China)
X. Fan, Prof. Y. Wang, Prof. Q. Ye
Zhongnan Hospital of Wuhan University
Institute of Hepatobiliary Diseases of Wuhan University
Wuhan, 430071 (China)

[**] This work was supported by National Basic Research Program of China (973 Program, grant number 2010CB732203), the Major Program of National Natural Science Foundation of China (grant number 21334005) and the National Natural Science Foundation of China (grant number 20874079).

Supporting information for this article is available on the WWW under http://dx.doi.org/10.1002/anie.201412129.

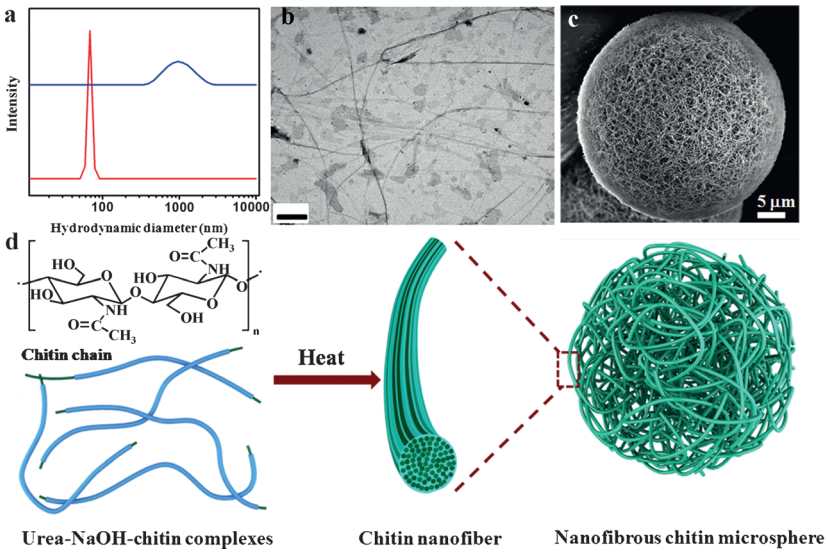

Figure 1. a) Hydrodynamic diameter distribution of the dilute chitin solution (0.01 wt%) with dynamic light scattering before (red) and after (blue) heating at 60 °C for 2 minutes. b) TEM image of this chitin nanofiber (blue; scale bar = 500 nm). c) Nanofibrous microspheres consisting of the chitin nanofibers (scale bar = 5 μm). d) A schematic of the fabrication of the nanofibrous microspheres self-assembled from chitin in the urea–NaOH–chitin complex solution.

to longer nanofibers (reaching several mirometers). In the hydrodynamic diameter distribution pattern measured by dynamic light scattering (Figure 1a), a peak of the NaOH hydrogen-bonded chitin complex in a very diluted solution appeared at 65 nm before heating, and a broader peak at 900 nm, corresponding to chitin aggregates including nanofibers and their networks (Figure 1b), was observed after heating. This further confirmed that chitin chains self-assembled to form nanofibers at elevated temperature. The representative nanofibrous microspheres (NCM; Figure 1c) were constructed from a chitin-concentrated solution (7 wt%) using a "bottom-up" fabrication method. The chitin solution was emulsified into liquid microspheres in isooctane with the surfactants Tween-85 and Span 85 under rigorous stirring at 0 °C. Subsequently, the mixture was treated with a 60 °C bath to rapidly induce the formation of chitin nanofibers, which formed weaved microspheres within 2 minutes. A schematic of the fabrication of the nanofibrous chitin microspheres is proposed in Figure 1d. The nanofibers consisted of the chitin chains entangled and cross-linked with each other to construct the microspheres. In our findings, the chitin dissolution and preparation of the nanofibrous microspheres all were physical processes, retaining the intrinsic structure and inherent bioactivity of chitin.[16a–d] Figure 2 shows the SEM images of the nanofibrous chitin microspheres and their size distribution. The nanofibers with an average diameter of about 26 ± 5 nm and at least several micrometer lengths formed weaved microspheres with a relatively narrow size distribution from 15 to 65 μm. The microspheres had a uniform architecture throughout. Namely, both the surface and the fracture surface of the chitin microspheres had the same homogeneous nanofibrous architecture (Figure 2c–e). Moreover, the average size of the nanofibrous chitin microspheres was tunable from 3 to 130 μm by varying the oil/water ratio, surfactant amount, and stirring speed (Figure S2, Table S1). A higher stirring speed, and/or larger amount of surfactant, and/or oil/water ratio decreased the diameter of NCM (Table S1). Furthermore, the size of the microspheres observed by SEM was consistent with that of the optical microscopic measurements (Figure S2), suggesting that there was no obvious shrinkage of the spheres after freeze-drying. In particular, the nanofibrous chitin microspheres displayed a well-distributed apparent porous structure (200–900 nm). Moreover, the NCM microspheres had a specific surface area of 294 $m^2 g^{-1}$ determined from nitrogen adsorption and desorption isotherms (Figure S3), as well as an IUPAC type I H3 hysteresis loop. The Barrett–Joyner–Halendar (BJH) analysis indicated that the nanofibrous microspheres had a maximum pore size distribution at proximately 25 nm at mesoporous scale. The microspheres had a similar degree of acetylation (DA = 89%) and the same α-chitin crystalline structure [but an obviously lower crystallinity of 41% compared with the original chitin (DA = 93%, crystallinity 72%); Figures S4 and S5]. Interestingly, the diameter of the chitin nanofibers and spherical structure of the chitin microspheres could be tuned by changing the chitin solution concentration and the treatment temperature. Specially, at the lowest concentration (3 wt%), most of the chitin micro-

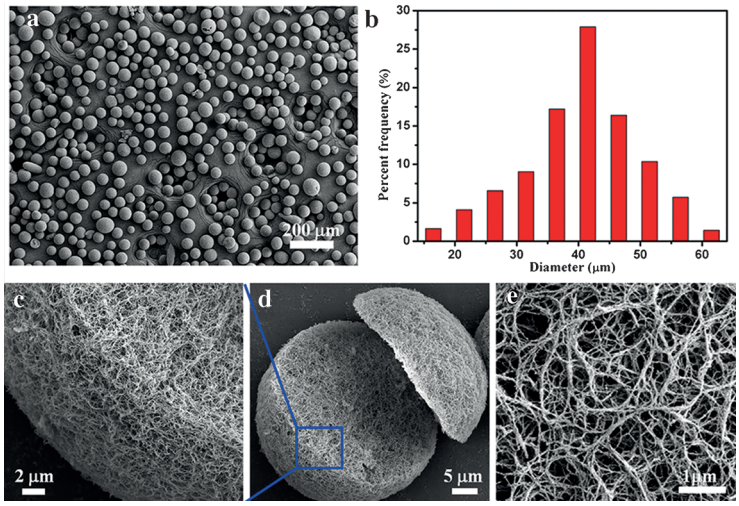

Figure 2. a) SEM image of the nanofibrous chitin microspheres (scale bar = 200 μm) and b) its size distribution. c,d) SEM image of a representative cross-section of nanofibrous chitin microspheres (the scale bars are 2 and 5 μm, respectively). e) A high-magnification SEM image of the surface of a nanofibrous chitin microsphere (scale bar = 1 μm).

spheres exhibited a shriveled spherical shape with a looser surface (Figure S6). With an increase in the chitin concentration, more perfect and denser microspheres were obtained, however, the size distribution of the microsphere (Figure S6a1–e1) and the diameter of the nanofibers changed hardly (Figure S6a5–e5). The entangled and cross-linked nanofibrous and porous structure existed throughout the chitin microspheres (Figure S6a4–e4). A chitin solution of low concentration resulted in a relatively loose surface compared with that of a highly concentrated solution (Figure S6a3–e3). The probable explanation for the different morphology was that the relatively low density of the chitin nanofibers could not strongly prop up the microspheres.

Furthermore, by fixing the chitin concentration (7 wt%), the nanofiber size and spherical shape of the nanofibrous chitin microsphere could be controlled by changing the temperature. At relatively low temperature (10°C), the urea–NaOH–chitin complex was destroyed slowly, leading to the partial peeling off of the urea–NaOH sheath attached on the chitin chains, resulting in imperfect chitin bundles and damaged microspheres (Figure S7a1,a2). On the contrary, at elevated temperature the urea–NaOH–chitin complex was destroyed completely to induce an extremely fast aggregation to freeze the self-assembled chitin nanofibers, leading to perfect chitin microspheres (Figure S7f1,f2), as a result of the strong tendency of aggregation caused by the sufficient hydrogen bonding between chitin chains. Moreover, the regeneration temperature also significantly affected the diameter of the nanofibers in the chitin microspheres (Figure S7a2–f2). As shown in Figure 3, the average diameter of a chitin nanofiber decreased from 42 to 26 nm at an increase

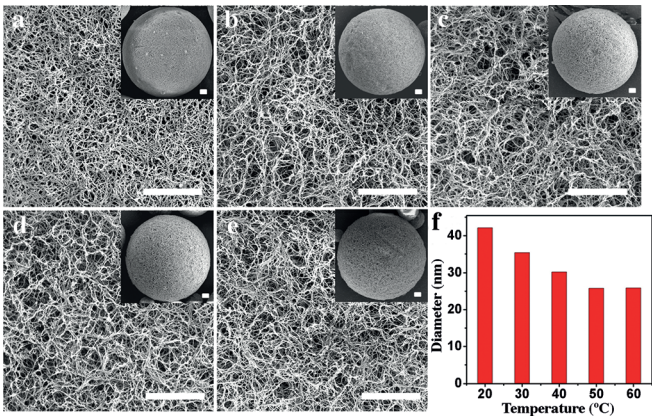

Figure 3. SEM image of the surface of the nanofibrous chitin microspheres fabricated at a) 20, b) 30, c) 40, d) 50, and e) 60°C; The Insets illustrates the morphology the nanofibrous chitin microspheres. f) The diameter size distribution of the single chitin nanofibers on the chitin microspheres. The scale bar is 5 μm.

in temperature from 20 to 60°C. At low temperature, the partly broken urea–NaOH–chitin complex still possessed some mobility to attach to each other to form the loose nanofibers with larger diameters. However, at high temperature, the NaOH/urea sheath around the chitin chains was destroyed quickly and completely. The large amounts of exposed hydroxy groups accelerated the rearrangement of the chitin chains through hydrogen bonding as well as hydrophobic interactions, which resulted in a stronger thermodynamic driving force for the self-aggregation of chitin chains in a parallel way to form the relatively tight nanofibers.

To evaluate the use of the chitin microspheres in the 3D liver scaffolding, an immortal normal human hepatic cell line L02 was selected as the model to test the attachment and biocompatibility, because of its ability to overcome the shortage of primary hepatocytes (also difficult to proliferate in vitro) for liver tissue engineering and retain the hepatic activity in vitro.[18] The flow cytometry and fluorescence microscopy (Figure S8) showed that the L02 cells could adhere and proliferate on the surface of the NCM chitin microspheres, indicating their excellent biocompatibility. Additionally, the magnetic microgels have received considerable attention in medicine applications such as directing cellular manipulation and 3D cell culture, as well as active targeting in drug delivery.[19] Thus, the magnetic chitin microspheres were fabricated by mixing Fe_3O_4 nanoparticles (NPs) with the chitin solution and then self-assembled by immediate treatment at high temperature. The resulting magnetic nanofibrous chitin microspheres (MNCM) not only displayed the same nanofibrous structure as the pure chitin microspheres (Figure S9), but also showed superparamagnetic behavior with an extremely small hysteresis loop, indicating the good magnetic response properties (Figure S10e). To evaluate the manipulation of MNCM by magnetic field in the cell culture application, a magnet bar was used to induce the MNCM cultured with L02 cells to assemble into a line geometry (Figure S10d). This indicated a great potential for target cell delivery. As shown in Figure 4a1, the MNCN enhanced the L02 cells adhesion and proliferation with the significant difference observed after 48 h. The cell viabilities reached up to 96% within 72 h (Figure 4a2), indicating a good biocompatibility of MNCM. The magnetic field was employed to maintain the accumulative line shape of the MNCM (Figure S10d) in the cell culture process. The bright field and fluorescence microscopy images (Figure 4a3,a4 and b4) indicated that the cells adhered and proliferated well on the surface and in the cavities among the nanofibrous microspheres. Interestingly, most MNCM still assembled together after the magnet was removed after 72 h of cell culture. The cells proliferated in the cavities among the MNCM and glued the microspheres together, suggesting a cohesive force (Figure 4a3,a4). From the SEM images (Figure 4b1–b3), a clearer insight of the interaction between cells and MNCM appeared. The cells filopodium extended and adhered on the nanofibers of the peripheral microspheres and then glued the MNCM together (Figure 4b2,b3 and Figure S11). Therefore, the chitin nanofibers played an important role in the enhancement of the adhesion of the cells. Moreover, the cells exhibited a 3D adhesion and proliferation on MNCM, which was critical for cell microcarrier and 3D scaffolding applications. Chitin is intrinsically a part of living organisms, and it shows biocompatibility and is anti-bacterial, as well as it facilitates the exposure of DNA to the cell surface.[20] These exploratory cell experiments proved that the nanofibrous chitin microspheres could indeed

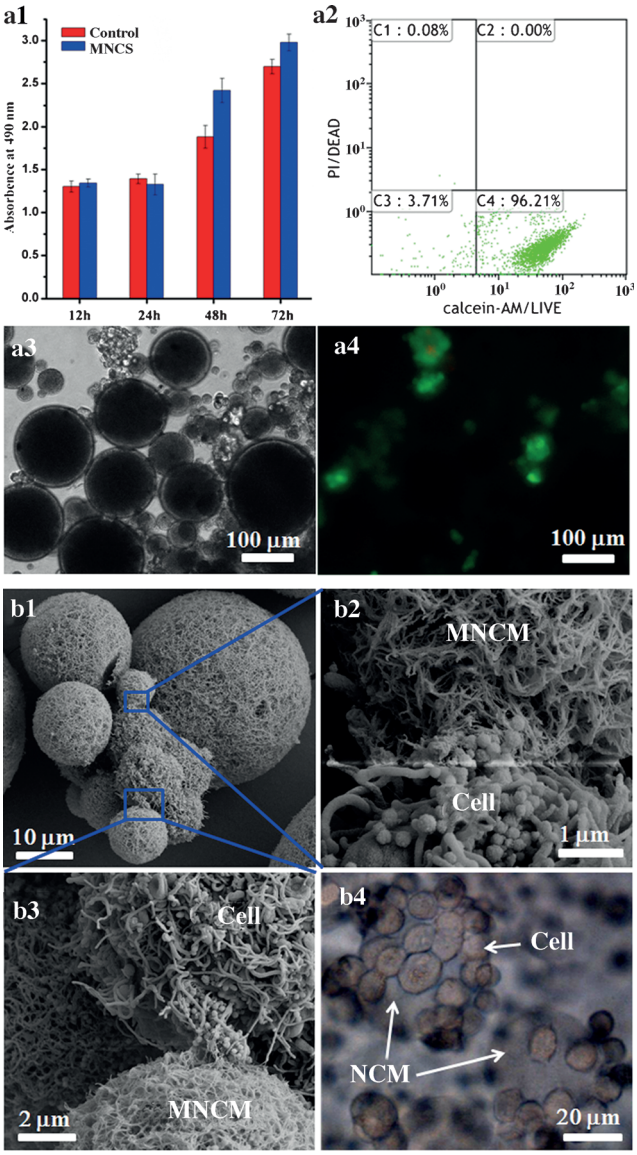

Figure 4. a1) MTT assay (MTT = 3-(4,5-dimethylthiazol-2-yl)-2,5-diphenyltetrazolium bromide) for the cell viability on magnetic nanofibrous chitin microspheres. a2) Flow cytometry for 72 h. Cell viability staining was performed with calcein AM/propidium iodide (live/dead assay kit, Invitrogen), a3) bright field and a4) live/dead assay fluorescent image of L02 cultured on the magnetic nanofibrous chitin microspheres (green represents live cells, red represents dead cells). b1–b3) SEM images and b4) optical photomicrographs of L02 cultured on magnetic (b1–b3) and pure (b4) chitin microspheres, respectively.

support cells well and showed the high attachment efficiency, as a result of their nanofibrous architecture and the inherent biocompatibility of chitin. Moreover, the abundant cavities in the microspheres benefited from the transportation of nutrients, and removal of metabolic byproducts. Therefore, the nanofibrous microspheres are potentially useful as 3D tissue-engineering materials.

In summary, a facile method for the construction of nanofibrous microspheres from chitin in NaOH/urea aqueous solution through thermally induced self-assembly was reported for the first time. At relative high temperatures, the chitin chains in the NaOH/urea aqueous solution rapidly self-aggregated in parallel to form nanofibers, which then formed weaved microspheres by a "bottom-up" fabrication method. Both the surface and fracture surface of the chitin microspheres showed the same homogeneous nanofibrous architecture throughout and a large specific surface area. Particularly, the size and structure of the microspheres could be tuned by changing the fabrication parameters, temperature and chitin concentration. The exploratory cell experiments proved that the nanofibrous chitin microspheres could indeed support cells well. Cells could also adhere to the chitin microspheres containing the iron oxide nanoparticles, and showed a high attachment efficiency. Therefore, the microspheres are promising candidates as excellent 3D cell carriers for applications in tissue engineering.

Keywords: cell microcarriers · chitin nanofibers · microspheres · nanofibrous architecture · self-assembly

How to cite: *Angew. Chem. Int. Ed.* **2015**, *54*, 5152–5156
Angew. Chem. **2015**, *127*, 5241–5245

[1] a) M. A. Correa-Duarte, N. Wagner, J. Rojas-Chapana, C. Morsczeck, M. Thie, M. Giersig, *Nano Lett.* **2004**, *4*, 2233–2236; b) S. Ryu, C. Lee, J. Park, J. S. Lee, S. Kang, Y. D. Seo, J. Jang, B.-S. Kim, *Angew. Chem. Int. Ed.* **2014**, *53*, 9213–9217; *Angew. Chem.* **2014**, *126*, 9367–9371; c) S. W. Crowder, D. Prasai, R. Rath, D. A. Balikov, H. Bae, K. I. Bolotin, H.-J. Sung, *Nanoscale* **2013**, *5*, 4171–4176.
[2] X. Liu, X. Jin, P. X. Ma, *Nat. Mater.* **2011**, *10*, 398–406.
[3] a) V. Chaurey, F. Block, Y.-H. Su, P.-C. Chiang, E. Botchwey, C.-F. Chou, N. S. Swami, *Acta Biomater.* **2012**, *8*, 3982–3990; b) B. V. Slaughter, S. S. Khurshid, O. Z. Fisher, A. Khademhosseini, N. A. Peppas, *Adv. Mater.* **2009**, *21*, 3307–3329.
[4] a) P. Zorlutuna, N. Annabi, G. Camci-Unal, M. Nikkhah, J. M. Cha, J. W. Nichol, A. Manbachi, H. Bae, S. Chen, A. Khademhosseini, *Adv. Mater.* **2012**, *24*, 1782–1804; b) H. Sekine, T. Shimizu, K. Sakaguchi, I. Dobashi, M. Wada, M. Yamato, E. Kobayashi, M. Umezu, T. Okano, *Nat. Commun.* **2013**, *4*, 1399; c) Z. Chen, W. Ren, L. Gao, B. Liu, S. Pei, H.-M. Cheng, *Nat. Mater.* **2011**, *10*, 424–428.
[5] a) M. E. Kolewe, H. Park, C. Gray, X. Ye, R. Langer, L. E. Freed, *Adv. Mater.* **2013**, *25*, 4459–4465; b) Y. S. Zhang, X. Cai, J. Yao, W. Xing, L. V. Wang, Y. Xia, *Angew. Chem. Int. Ed.* **2014**, *53*, 184–188; *Angew. Chem.* **2014**, *126*, 188–192; c) A. Jain, M. Betancur, G. D. Patel, C. M. Valmikinathan, V. J. Mukhatyar, A. Vakharia, S. B. Pai, B. Brahma, T. J. MacDonald, R. V. Bellamkonda, *Nat. Mater.* **2014**, *13*, 308–316; d) P. Fattahi, G. Yang, G. Kim, M. R. Abidian, *Adv. Mater.* **2014**, *26*, 1846–1885.
[6] a) Y. T. Matsunaga, Y. Morimoto, S. Takeuchi, *Adv. Mater.* **2011**, *23*, H90–H94; b) J. Fang, Y. Zhang, S. Yan, Z. Liu, S. He, L. Cui, J. Yin, *Acta Biomater.* **2014**, *10*, 276–288.
[7] Y. Man, P. Wang, Y. Guo, L. Xiang, Y. Yang, Y. Qu, P. Gong, L. Deng, *Biomaterials* **2012**, *33*, 8802–8811.
[8] C. K. S. Pillai, W. Paul, C. P. Sharma, *Prog. Polym. Sci.* **2009**, *34*, 641–678.
[9] a) C. Zhong, A. Kapetanovic, Y. Deng, M. Rolandi, *Adv. Mater.* **2011**, *23*, 4776–4781; b) J.-i. Kadokawa, A. Takegawa, S. Mine, K. Prasad, *Carbohydr. Polym.* **2011**, *84*, 1408–1412; c) W. Suginta, P. Khunkaewla, A. Schulte, *Chem. Rev.* **2013**, *113*, 5458–5479; d) M. Rinaudo, *Prog. Polym. Sci.* **2006**, *31*, 603–632.
[10] a) S. Ifuku, H. Saimoto, *Nanoscale* **2012**, *4*, 3308–3318; b) S. Ifuku, M. Nogi, K. Abe, M. Yoshioka, M. Morimoto, H. Saimoto, H. Yano, *Biomacromolecules* **2009**, *10*, 1584–1588; c) J. Wu, J. C.

Meredith, *ACS Macro Lett.* **2014**, *3*, 185 – 190; d) S. W. Choi, J. Xie, Y. Xia, *Adv. Mater.* **2009**, *21*, 2997 – 3001.
[11] M. Poirier, G. Charlet, *Carbohydr. Polym.* **2002**, *50*, 363 – 370.
[12] H. Tamura, H. Nagahama, S. Tokura, *Cellulose* **2006**, *13*, 357 – 364.
[13] X. Hu, Y. Du, Y. Tang, Q. Wang, T. Feng, J. Yang, J. F. Kennedy, *Carbohydr. Polym.* **2007**, *70*, 451 – 458.
[14] S. S. Silva, A. R. C. Duarte, J. F. Mano, R. L. Reis, *Green Chem.* **2013**, *15*, 3252.
[15] a) C. Zhong, A. Cooper, A. Kapetanovic, Z. Fang, M. Zhang, M. Rolandi, *Soft Matter* **2010**, *6*, 5298 – 5301; b) P. Hassanzadeh, W. Sun, J. P. de Silva, J. Jin, K. Makhnejia, G. L. W. Cross, M. Rolandi, *J. Mater. Chem. B* **2014**, *2*, 2461; c) P. Hassanzadeh, M. Kharaziha, M. Nikkhah, S. R. Shin, J. Jin, S. He, W. Sun, C. Zhong, M. R. Dokmeci, A. Khademhosseini, M. Rolandi, *J. Mater. Chem. B* **2013**, *1*, 4217 – 4224; d) A. Cooper, C. Zhong, Y. Kinoshita, R. S. Morrison, M. Rolandi, M. Zhang, *J. Mater. Chem.* **2012**, *22*, 3105 – 3109.
[16] a) C. Chang, S. Chen, L. Zhang, *J. Mater. Chem.* **2011**, *21*, 3865 – 3871; b) Y. Huang, Z. Zhong, B. Duan, L. Zhang, Z. Yang, Y. Wang, Q. Ye, *J. Mater. Chem. B* **2014**, *2*, 3427 – 3432; c) M. He, Z. Wang, Y. Cao, Y. Zhao, B. Duan, Y. Chen, M. Xu, L. Zhang, *Biomacromolecules* **2014**, *15*, 3358 – 3365; d) B. Ding, J. Cai, J. Huang, L. Zhang, Y. Chen, X. Shi, Y. Du, S. Kuga, *J. Mater. Chem.* **2012**, *22*, 5801 – 5809; e) B. Duan, F. Liu, M. He, L. Zhang, *Green Chem.* **2014**, *16*, 2835 – 2845; f) B. Duan, C. Chang, B. Ding, J. Cai, M. Xu, S. Feng, J. Ren, X. Shi, Y. Du, L. Zhang, *J. Mater. Chem. A* **2013**, *1*, 1867 – 1874.
[17] Y. Fang, B. Duan, A. Lu, M. Liu, H. Liu, . Xu, L. Zhang, *Biomacromolecules* **2015**, submitted.
[18] a) A. J. Strain, J. M. Neuberger, *Science* **2002**, *295*, 1005 – 1009; b) X. Hu, T. Yang, C. Li, L. Zhang, M. Li, W. Huang, P. Zhou, *Transplant. Proc.* **2013**, *45*, 695 – 700; c) Z. Ding, J. Chen, S. Gao, J. Chang, J. Zhang, E. T. Kang, *Biomaterials* **2004**, *25*, 1059 – 1067; d) W.-Q. Xiang, W.-F. Feng, W. Ke, Z. Sun, Z. Chen, W. Liu, *J. Hepatol.* **2011**, *54*, 26 – 33; e) M.-c. Chen, Y.-y. Ye, G. Ji, J.-w. Liu, *J. Agric. Food Chem.* **2010**, *58*, 3330 – 3335.
[19] a) Y. Li, G. Huang, X. Zhang, B. Li, Y. Chen, T. Lu, T. J. Lu, F. Xu, *Adv. Funct. Mater.* **2013**, *23*, 660 – 672; b) G. R. Souza, J. R. Molina, R. M. Raphael, M. G. Ozawa, D. J. Stark, C. S. Levin, L. F. Bronk, J. S. Ananta, J. Mandelin, M.-M. Georgescu, J. A. Bankson, J. G. Gelovani, T. C. Killian, W. Arap, R. Pasqualini, *Nat. Nanotechnol.* **2010**, *5*, 291 – 296; c) F. Xu, C.-a. M. Wu, V. Rengarajan, T. D. Finley, H. O. Keles, Y. Sung, B. Li, U. A. Gurkan, U. Demirci, *Adv. Mater.* **2011**, *23*, 4254 – 4260.
[20] a) D. H. Bartlett, F. Azam, *Science* **2005**, *310*, 1775 – 1777; b) T. Liu, Z. Liu, C. Song, Y. Hu, Z. Han, J. She, F. Fan, J. Wang, C. Jin, J. Chang, J.-M. Zhou, J. Chai, *Science* **2012**, *336*, 1160 – 1164.

Received: December 17, 2014
Revised: January 22, 2015
Published online: February 25, 2015

